Hindawi
Advances in Civil Engineering
Volume 2020, Article ID 8392935, 16 pages
https://doi.org/10.1155/2020/8392935

Research Article

Effect of Straw Fiber Modification Methods on Compatibility between Straw Fibers and Cement-Based Materials

Demin Jiang,[1] **Penghui An**,[1] **Suping Cui**,[2] **Shiguo Sun**,[1] **Jingzong Zhang**,[1] **and Tianfu Tuo**[1]

[1]*College of Civil Engineering, North China University of Technology, Beijing 100144, China*
[2]*College of Materials Science and Engineering, Beijing University of Technology, Beijing 100124, China*

Correspondence should be addressed to Demin Jiang; jdm2004@126.com

Received 12 September 2019; Revised 6 December 2019; Accepted 20 December 2019; Published 31 January 2020

Academic Editor: Chongchong Qi

To improve the utilization of crop straws as a resource and the compatibility between straw fibers and cement-based materials, the hydration of modified straw fiber cement-based composite (SFCC) was studied. The structural characteristic of SFCC was investigated by FTIR, SEM, and XRD. The results show that the setting time of several modified straw fiber SFCC pastes was shorter than that of the unmodified straw fiber SFCC paste, and the best method of fiber modification to improve the setting time of the SFCC paste is $Na_2O{\cdot}nSiO_2$ treatment. The recommended fiber modification method for improving the compatibility between straw fibers and cement-based materials is alkali modification, followed by pure acrylic emulsion modification and $Na_2O{\cdot}nSiO_2$ modification. To improve the strength of SFCC, the straw fiber should be modified by alkali, followed by pure acrylic emulsion and $Na_2O{\cdot}nSiO_2$ modification and the method of water modification is also recommended. The phase types and relative contents of crystalline hydration products mixed with the modified straw fiber SFCC are significantly higher than those of the unmodified fiber SFCC. The fiber treatment method that was most helpful to increase the structural density of hydrates of SFCC was alkali treatment and pure acrylic emulsion treatment, followed by $Na_2O{\cdot}nSiO_2$ treatment.

1. Introduction

Cement-based materials possess some shortcomings, such as low tensile strength, poor toughness, and difficult control of crack width after cracking. To overcome these disadvantages, it is advisable to use a kind of composite material, a fiber-reinforced cement-based composite (also called fiber-reinforced cement-based composite), composed of discontinuous short fibers or continuous long fibers mixed with cement-based materials as reinforcing materials [1–3]. At present, the main reinforcements in fiber-reinforced cement-based composites are steel fibers, synthetic polymer fibers, carbon fibers, glass fibers, and asbestos fibers [4–6]. However, the problem of the corrosion of steel fibers, the harmful production process of synthetic polymer fibers, and the possibility of pathogenicity of glass fibers have not been well solved [7, 8]. Thus, the poor economy and environmental problems related with the use of these fibers cannot be ignored. With the continuous progress of science and technology and the improvement in people's living standards, a new type of lightweight, high strength, energy-saving, environment friendly, recyclable, and low carbon building material is urgently required. And the newly emerged plant fiber cement-based composites (PFCC) with natural plant fibers as reinforcing materials are precisely one of the very representative building materials to meet these requirements [9–11]. Because of its low cost, abundance, and ecofriendliness, an increasing number of institutions in many countries and regions have showed a strong interest in research of plant fiber cement-based composite materials and achieved remarkable results [12–15].

The straw is the general name of the stem and leaf (ear) of ripe crops, usually referring to the remaining part of the crops, or the waste of the crops, when wheat, rice, corn, potatoes, rape, cotton, sugar cane, and other crops are harvested. Crop straw is one of the most abundant materials in the world. According to statistics, the output of

straw in the world is more than 2.9 billion tons every year, including 21% wheat straw, 19% rice straw, 10% barley straw, 35% corn straw, 2% rye straw, 3% oat straw, 5% cereal straw, and 5% sorghum straw. 66% of the world's crop straw is returned directly to the field or burned as live energy, 19% is used as building materials or covering materials in vegetable production, 12% as forage for herbivorous livestock, and about 3% as raw materials for handicrafts [16–18]. China is a big agricultural country, which grows a large amount of crops every year, thus producing abundant agricultural waste. According to statistics, China produces more than 700 million tons of crop straw every year, ranking first in the world, with the straw of rice, corn, and wheat being the three major grain crops with the largest output of straw, accounting for 75.6% of the total straw resources, i.e., 210 million tons, 209 million tons, and 110 million tons, respectively [19, 20]. When crops are harvested, part of the crop straw is used for feeding livestock, returning to the field, making crafts, and other purposes, while the rest is simply burned or piled up or discarded at will. This treatment not only wastes valuable natural resources, but also pollutes the environment, posing a major public hazard. Therefore, it is urgent to find a more reasonable way to treat crop straw, and the use of crop straw to prepare PFCC will be the most effective way to utilize straw resources.

Although PFCC has many advantages, such as energy saving, environmental friendliness, high toughness, and abundance, there are still many problems in its application because of its low strength, poor durability, and other disadvantages, of which the poor compatibility between plant fibers and cement remains a difficult problem affecting its promotion and application both at home and abroad [21, 22]. The poor compatibility between plant fibers and cement-based materials is mainly reflected in the following aspects: firstly, the dissolution of the plant fiber in a cement hydration environment (called extract) has a hindrance effect on cement hydration; secondly, a large amount of polar hydroxyl groups existing in plant fibers have high water absorption, which will increase the amount of water needed for the PFCC mixture to reach the same density level in the product molding process, having a detrimental effect on the physical and mechanical properties of PFCC [23–25]; thirdly, the alkaline erosion of plant fibers in cement hydrates will greatly decrease the strength and durability of plant fibers. Therefore, in order to improve the compatibility between plant fibers and cement-based materials, it is necessary to modify plant fibers before use. Although many achievements have been made on the compatibility between vegetable fibers and cement-based materials [26, 27], the pertinence and practicability of the modification methods of vegetable fibers still need to be further explored, and there is not much literature on the comprehensive evaluation of the effect of modified fibers on the compatibility of cement-based materials.

The straw used in this study is one of the most abundant raw materials in China, and the straw fibers are taken as this study's research object. So, a variety of modification materials and different modification technologies were used to modify the straw fibers to study the effect of different modification methods on the hydration properties of straw fiber cement-based composites (SFCC). In addition, FTIR, XRD, and SEM were used to characterize the chemical structure, mineral composition, and micromorphology of hardened SFCC. The results of this study will provide a theoretical and scientific basis for improving the compatibility between straw fibers and cement-based materials and promoting the comprehensive utilization of straw.

2. Materials and Methods

2.1. Materials

2.1.1. Cementitious Material. Cement: Grade 42.5 common Portland cement of Diamond Brand was manufactured by Yanjiao New Building Materials Co., Ltd., Sanhe City, Hebei Province. The chemical compositions of cement and fly ash are shown in Table 1, and their particle size distribution and fineness are shown in Table 2.

Fly ash: Class II fly ash was purchased from the Shijingshan Power Plant, and its performance meets the requirements of the Chinese standard GB/T 50146-2014 (Technical Code for Application of Fly Ash Concrete).

2.1.2. Straw Stalk. Straw stalk was purchased from Allan Shipping Services Co., Ltd., Rizhao, Shandong Province. The straw stalks were dried by an electric blast drying oven at $85 \pm 1^{\circ}C$, crushed by a universal crusher [28], and then divided into fibers with different particle sizes by a 0.15–0.475 mm sieve. The 0.15–0.3 mm fibers were used as raw material for the test [22, 29]. The appearance of straw and straw fibers is shown in Figure 1. The bulk density of straw fibers is 0.13 g/cm^3, the apparent density is 0.17 g/cm^3, and the chemical composition is shown in Table 3.

2.1.3. Modifier of Straw Fibers

Sodium silicate solution ($Na_2O{\cdot}nSiO_2$): manufactured by Beijing Yongfei Adhesive Factory; modulus 3.1, Baume 40°, density 1.38 g/cm^3, and content of total solids 36.20%.

Pure acrylic polymer emulsion: PRIMAL MAC-261P acrylic by Rohm & Haas, USA, with a solid content of 50%, a density of 1.04 g/cm^3, and a pH value of 8.8.

Silicone waterproof emulsion: IE-6683 waterproof emulsion, alkoxy silane, and PDMS (polydimethylsiloxane) developed by Dow Corning, USA, with an active material content of 40%, a density 1.01 g/cm^3, and pH 6–8.

Sodium hydroxide (NaOH): produced by Beijing Chemical Plant, AR; content of major ingredients ≥96.0%.

Water: drinking water meeting the China national standards, i.e., pH = 6.91 at 25°C.

Table 1: Chemical composition of cement and mineral admixtures (mass fraction, %).

Type of materials	CaO	SiO_2	Al_2O_3	Fe_2O_3	TiO_2	MgO	SO_3	Na_2O	Ignition loss
Cement	62.38	25.52	6.15	3.27	0.57	1.54	1.65	0.21	2.87
Fly ash	1.93	54.88	32.12	4.28	—	1.45	1.46	—	3.82

Table 2: Particle size distribution and fineness of cement and mineral admixtures (cumulative fraction, %).

Particle size (μm)	0.5	1.0	2.0	5.0	10.0	20.0	45.0	75.0	100.0	200.0	Fineness (m^2/kg)
Cement	0.60	4.24	7.05	17.13	36.89	65.07	97.42	100.00	—	—	389.2
Fly ash	0.33	1.92	2.93	7.93	20.23	40.23	69.65	86.05	93.77	100.00	217.4

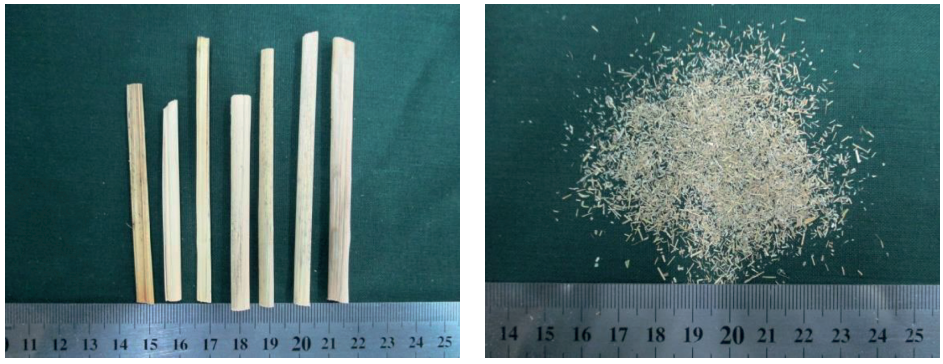

(a) (b)

Figure 1: Appearance of straw and straw fibers: (a) straw stalk; (b) straw fibers (particle size 0.3 mm).

Table 3: Chemical composition of straw fibers (%).

Moisture content	Ash content	Holocellulose	Cellulose	Pentosan	Lignin	Extracts of different solutions			
						Hot water	Cold water	Alcohol benzene	1% NaOH
5.06	15.35	62.41	39.27	17.93	17.35	14.97	11.96	9.72	51.26

The data were determined in accordance with the Test Method of GB/T 2677 for related ingredients of paper-making raw materials. Holocellulose is the sum of cellulose and hemicellulose in plant fiber raw materials, also known as total cellulose.

2.2. Methods

2.2.1. Pretreatment of Straw Fibers. In order to reduce the retarding effect of the straw fiber extract on cement and to reduce the water absorption of the straw fiber and improve the alkali resistance of the straw fiber, the method of coating the surface of the straw fiber with a protective film or pre-extracting straw the fiber extract can be used. After many years of early research, we found that the water glass solution can penetrate into the cracks and pores on the surface of the material, so as to block the cracks on the surface of the material, improve the overall density and strength of the material, and then improve the overall weathering resistance of the material. Pure acrylic polymer emulsion is an important film-forming material for exterior wall coatings. It has excellent water resistance, weatherability, and corrosion resistance. Silicone waterproof emulsion is a hydrophobic impermeable waterproof agent for porous material surface waterproofing treatment and has good water and alkali resistance. Alkali treatment can dissolve part of pectin, lignin, hemicellulose, and low-molecular impurities in the plant fiber, which is an effective method to remove the extract of the plant fiber. In order to reduce the environmental pollution caused by lye, it is also worth trying to use the water treatment plant fiber [22]. Therefore, three physical methods and two chemical methods were used to modify the straw fiber. The three physical methods were to spray a thin layer of three modifiers (i.e., sodium silicate solution, pure acrylic polymer emulsion, and silicon waterproof emulsion) to the surface of the straw, respectively. For smooth spraying and uniform coating, the sodium silicate solution and pure acrylic emulsion were diluted with pure water at a ratio of 1 : 1 and silicone waterproof emulsion was diluted with pure water at a ratio of 1 : 8. Spraying was performed in such a way that emulsion dampened fiber surfaces without any overflow. It is recommended that the above three diluted modifies account for 112.23%, 86.09%, and 78.69% of the straw fiber quality, respectively. Then the sprayed fibers were put into an electric blast drying oven and dried at 85 ± 1°C for 24–30 h, cooled to room temperature, and then stored in sealed plastic bags for use. Two chemical methods were dipping the straw fibers in sodium hydroxide (NaOH) solution with a mass density of 3% and water,

respectively, at room temperature. The dipping time of the alkali solution and water was 4 h and 10 h, respectively. When the dipped straw fibers were washed with water 5–7 times, they were dried in an electric blast drying oven at 85 ± 1°C for 24–30 h, and then they were cooled to room temperature and stored in sealed plastic bags for use.

2.2.2. Test of Straw Fiber Water Absorption. The test was performed in accordance with the lightweight aggregate water absorption testing methods of the Construction Industry Standard JGJ 51-2002: Technical Specifications for Lightweight Aggregate Concrete. 5 grams of fiber samples were placed into a 0.08 mm square-hole sieve and placed into a basin. Water level did not exceed the height of the sieve frame. The square-hole sieve was taken out of the basin at intervals of one hour to wipe the bottom and the frame with a wrung wet towel, and fiber moisture in the sieve was blotted. Then, fibers were weighed with an electronic scale, and water absorption of the fiber mass was calculated according to the following formula:

$$w_t = \frac{m_t - m_0}{m_o} \times 100\%, \quad (1)$$

where w_t represents water absorption (%) when the immersion time was t, m_t represents fiber mass (g) when the immersion time was t, and m_0 represents fiber mass (g) when fibers were dried to a constant weight before immersion.

2.2.3. Test of SFCC Paste Setting Time. The test was performed in accordance with the "Standard Cement Consistency Water Consumption, Setting Time, Stability Test Methods (Substitution)" of GB/T1346-2011. Material proportion of the sample: the base group without the fiber group: 270 g cement, 30 g fly ash, and 93 ml water; the cementitious material of the fiber group was the same as that of the base group: 60 g straw fiber content, and, considering the additional water consumption caused by fiber water absorption, the fiber group water consumption was 190 ml. In this study, only the final setting time was recorded, i.e., the time from the moment when water began to add to the moment when the touch needle sank into the paste and it should not exceed 0.5 mm.

2.2.4. Evaluation of Compatibility between Straw Fibers and Cement-Based Materials. The test was performed in accordance with the "Cement Hydration Heat Test Methods (Direct Method)" of GB/T 12959-2008 and related literature [30–32]. In the test, the SFCC mixture paste was put into an insulation barrel with a double-layer vacuum glass tank and the hydration temperature of the mixture was measured by a hand-held electronic thermometer. Material proportion of the sample: for the reference group, the cementitious material was 200 g (cement 180 g, fly ash 20 g) and the water was 90 ml; for the fiber blending group, the amount of the cementitious material was the same as that of the reference group and the content of the straw fiber was 20 g, and considering the additional water consumption caused by the water absorption of the fiber, the water was 100 ml. The measurement interval was 0.5 h within 24 h. Room temperature was 13 ± 1°C.

2.2.5. Analysis of Molecular Structure of Straw Fibers. In the test, a Tensor 27 Type FTIR (Fourier Transform Infrared Spectroscopy) manufactured by Bruker, Germany, was used for analysis. The scanning wave number range was set at 4000-400 cm^{-1}, the scanning frequency was 32 times, and the resolution was 4 cm^{-1}. The test sample was a translucent ingot sheet made of a mixture of straw fibers and KBr, i.e., 3.5 mg dry straw fibers and 350 mg dry KBr were mixed into an agate mortar and porphyrized. Then, 300 mg of the mixture was poured into a sheet die, and a uniform and translucent ingot was obtained at the pressure of 10 MPa for 1-2 minutes.

2.2.6. Test of SFCC Mechanical Properties. The test was performed in the light of "Testing Method for Strength of Cement Mortar (ISO Method)" of GB/T17671-1999, and the mixture consistency was tested in accordance with the "Testing Methods for Water Consumption, Setting Time, and Stability of Cement Standard Consistency" of GB/T1346-2011. A 300 kN electronic universal testing machine (CDT305, by Shenzhen, China) was used to test the flexural and compressive strength of specimens. Specimens' size: 40 mm × 40 mm × 160 mm. A group of specimens (three specimens) were taken out of each type of the modified straw fiber SFCC at each age to test their strength; at first, 3 specimens out of each group of specimens for a bending test, resulting in six fractured blocks for a compressive strength test. The ratio (mass ratio) was cement: fly ash: leaf fiber: water = 1 : 0.11 : 0.17 : 0.54. When mixing, the consistency of the mixture should be controlled at 30 ± 3 mm and a certain amount of water should be adjusted according to the consistency value.

2.2.7. Analysis of Composition of SFCC Hydrates. A Shimadzu XRD-7000 X-ray diffractometer (XRD) was used in the test. The working voltage was 40 kV, the working current was 30 mA, the scanning range was from 10 to 80 degrees, the step length was 0.02 degrees/step, and the speed was 2 degrees/min. The specimens were the ones with the mechanical properties identical to those of 28 days of age. First, the specimens were chiseled into small pieces or granules, hammered into powder with a hammer, and then further ground into fine powder with an agate abrasive bowl to allow the specimens to pass through a 0.075 mm square-hole sieve, and finally the powder was placed on a blind-hole slide and flattened to specimens. Since the content of the same phase is proportional to the intensity of its diffraction peak, in order to reduce the intensity error caused by the distortion, overlap, and loss of the diffraction line, the sum of the product of the peak intensity of the three main peaks of the phase and the half-height-width (i.e., the peak area) is used to represent the diffraction

intensity of the phase to characterize the relative content of the phases of SFCC hydration products.

2.2.8. Analysis of Microstructure of Straw Fibers. The SU8020 type cold field emission scanning electron microscope by Hitachi with a test voltage of 20 kV was used to observe the samples, which should be dried at $85 \pm 1^{\circ}C$ and treated with 30 s spraying.

2.2.9. Microscopic Analysis of SFCC Hydrates. A SIGMA thermal field emission scanning electron microscope (SEM) with the test voltage of 10 kV by Carl Zeiss NTS, Germany, was used for the test. The specimens were the ones with the mechanical properties identical with those of 28 days of age. Before the test, the specimens were dried at $85 \pm 1^{\circ}C$ and smashed into small 2 mm square pieces, and treated with 30 s spraying.

3. Results and Discussions

In order to express the experiment conveniently, the processing methods of straw fibers and the performance tests of straw fibers and SFCC are sorted and coded. The meaning of the test serial number and the test code is shown in Table 4.

3.1. Effect of Modification Methods on the Microstructure of Straw Fibers. The SEM image of the microstructure of the unmodified and modified straw fibers is shown in Figure 2.

Figure 2(a) shows that the outer surface of the straw fiber sheath is alternately arranged by the areas with orderly arrangement of the particulate matter (called particulate matter area) and the areas without the particulate matter (called nonparticulate matter area). On the surface of the unmodified straw fibers, there are turn up lamellae and granular crumbs. There are waxy coat and cuticle on the epidermis. The cuticle will affect the adhesion between straw fibers and cement-based materials. The inner epidermis is composed of orderly arranged parenchyma cells. On the surface and inside of straw fibers, there are a great number of pores and cracks of different size, which are easily invaded by water and corrosive mediums and will increase the water absorption of fibers.

Figure 2(b) shows that the surface of straw fibers modified by $Na_2O{\cdot}nSiO_2$ was coated with a layer of silica gel. The fragile matter in the turn up lamellae and granular crumbs on the fiber surface decreased, while the bundles and lumps increased. As a result, the small openings and cracks on the surface were mostly blocked by the silica gel, thus increasing the density of the fiber surface, which in turn will prevent moisture from permeating and improve fiber resistance to water and erosion.

As shown in Figure 2(c), a glossy polymer film was coated on the surface of the straw fibers modified by pure acrylic emulsion. The film wrapped up the turn up lamellae crumbs and particles and filled the cavities and pores of the fiber surface, thereby reducing the defects inside fibers and improving their integrity and water resistance and preventing the alkaline ions in the cement from migrating to fiber cavities. As a result, the fiber alkali corrosion resistance is improved, and the interfacial effect between the fiber surface and cement-based materials and the adhesion between the fibers and substrate is increased [33].

As shown in Figure 2(d), the surface of straw fibers modified by a waterproofing emulsion is similar to that in Figure 2(a). The cavities on the surface and inside the fibers are covered with a layer of silicon hydrophobic film. The presence of the silicone hydrophobic film has improved the hydrophobicity of the fibers and, to a certain extent, improved the alkali corrosion resistance of the fibers, but it may also reduce the interfacial adhesion between the fiber surface and cement-based materials and the strength of SFCC [34].

Figure 2(e) shows that the turn up lamellar tissues fell off the water-modified straw fibers and the waxy layer on the outer surface decreased, but some columnar cell walls inside the fibers were destroyed and exposed, revealing a large number of pores and cracks, of which some pores contained some lamellar and granular scraps. This indicates that the bunchy fiber structure was partially eroded and damaged. This is because the water-modified fibers have removed part of hemicellulose, lignin, and other substances and have also dissolved a small amount of fatty substances and simple carbohydrates, revealing part of the fiber inner layer, thus increasing the surface roughness and porosity of fibers. Therefore, this may increase the water absorption of the fiber to a certain extent, but it can also improve the interfacial adhesion between the fiber surface and cement-based materials and improve the strength of SFCC.

As shown in Figure 2(f), the alkali-modified straw fibers are somewhat similar to that in Figure 2(e), i.e., the lamellar and nubbly bodies on the fiber surface have been damaged to a certain extent, especially the tissues of parenchymatous cells on the inner surface have been severely damaged, the turn up lamellar tissues have fallen off, and there is no waxy layer on the surface. The fascicular structure of fiber cell walls was separated and some tissues have been damaged and fallen off, forming many cavities and fissures. This is because alkali modification has removed some cellulose, hemicellulose, and lignin of fibers and dissolved pentosan, resin acid, and glucuronic acid, resulting in serious surface damage inside and outside the fibers, thus increasing the surface roughness and porosity [35, 36]. Although this may increase the fiber water absorption to a certain extent, the increased roughness can improve the interfacial adhesion between the fiber surface and cement-based materials and improve the compatibility between fibers and cement-based materials.

From the analysis of the morphology of the unmodified and modified straw fibers in Figure 2, it can be seen that the main purpose of the surface spraying modification (as shown in Figures 2(b)–2(d)) is to form on the fiber surface of a covering film, which in turn will plug the open pores and cracks on the fiber surface, thus increasing the surface density and reducing water absorbability of fibers. The impregnation modification (as shown in Figures 2(e) and 2(f)) is mainly to remove the educts (extracts) from the

Table 4: The meanings of test serial number and test code.

Method of fiber treatment	Pure cement-based materials	Raw fiber untreated	Sodium silicate solution spraying	Pure acrylic polymer emulsion spraying	Organosilicon waterproof emulsion spraying	Water dipping	Lye dipping
Serial number	0	1 or (a)	2 or (b)	3 or (c)	4 or (d)	5 or (e)	6 or (f)

Test code: DN-setting time test of the SFCC paste; DS-straw fiber mass water absorption within 24 hours; DR-hydration heat test of the SFCC paste; DG-FTIR test of straw fibers; DQ-mechanical properties test of SFCC; DX-XRD test of SFCC hydration products.

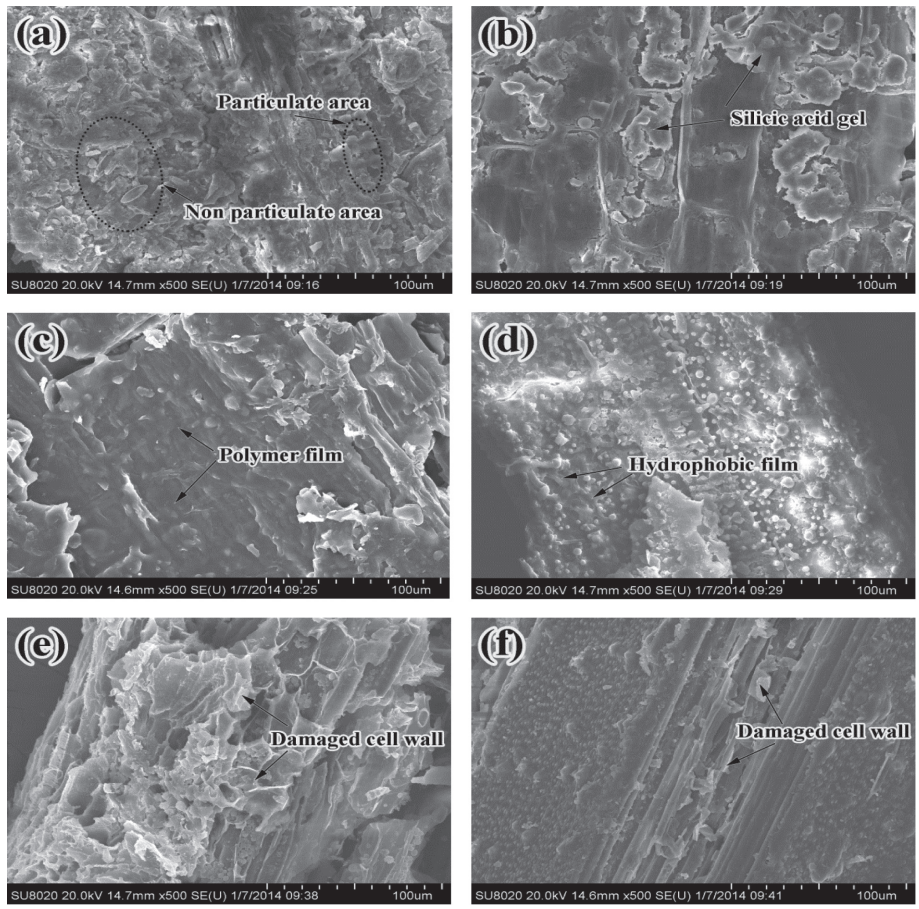

Figure 2: SEM images of straw fibers (500 times).

fibers, reducing the obstruction of the fibers to the hydration process of the SFCC paste. Although the two kinds of fiber modification methods differ in mechanisms, they can improve the compatibility between fibers and cement-based materials in different degrees or in different aspects, or improve the interfacial adhesion between fiber surface and cement-based materials, as well as the physical and mechanical properties of fiber-based cement-based materials. As shown in the microstructure of straw fibers, of all the straw fiber modification methods, alkali, $Na_2O{\cdot}nSiO_2$, and acrylic emulsion modifications are the best.

3.2. Effect of Modification Methods on Setting Time of SFCC Paste. The setting time (final setting time) of the FCC paste is shown in Figure 3. As shown in Figure 3, the DN0 of the base group sets the fastest, being 10 h. The setting time of the paste mixed with the straw fiber group is longer than that of the base group. The final setting time of DN1 blended with unmodified straw fibers is the longest, reaching 81.5 h, revealing a poor compatibility between unmodified straw fibers and cement-based materials. This is mainly because hemicellulose and a small amount of cellulose extracts in straw fibers affected the cement setting, for pentosan in hemicellulose is hydrolyzed into glucose and other monosaccharides in water or alkaline solution. These monosaccharides in the alkaline medium of cement are converted into glycic acid, which, together with the calcium ion of cement hydrates, produce calcium gluconate, which in turn, wraps around the cement particles, forming a shell, thus hindering the cement hydration [37, 38].

The setting time of several SFCC paste with modified straw fibers is shorter than that mixed with unmodified straw fibers, among which DN2 sets the fastest, being 12.5 h.

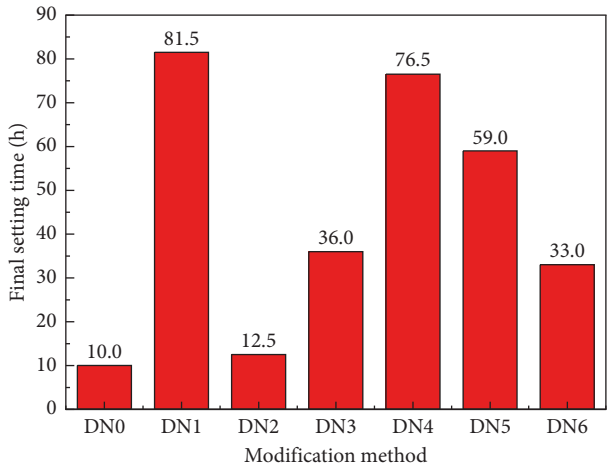

Figure 3: Final setting time of SFCC paste.

This is because after the modification of $Na_2O{\cdot}nSiO_2$, the amorphous silica gel generated on the surface of straw fibers can plug the pores on the fiber surface and form a hard shell on the fiber surface (see the response equation (2)), which reduces water absorption of the fibers and greatly reduces the overflow of anticoagulant components in straw fibers in the hydration process of the cement. At the same time, sodium silicate is a kind of concrete accelerator. The sodium silicate ($Na_2O{\cdot}nSiO_2$) adsorbed on the fiber surface takes part in the cement hydration process. The silicic acid produced by its hydrolysis reacts with calcium hydroxide resulted from hydrolysis of cement minerals to form hydrated calcium silicate ($3CaO{\cdot}SiO_2{\cdot}3H_2O$) which is insoluble in water (see the response equation (3)) [39], which destroys the hydrolysis equilibrium of tricalcium silicate and dicalcium silicate, thus resulting in the formation of a large amount of hydrated calcium silicate in a short time, making the SFCC paste rapidly set and harden.

$$Na_2O{\cdot}nSiO_2 + CO_2 + mH_2O = Na_2CO_3 + nSiO_2{\cdot}mH_2O \quad (2)$$

$$SiO_2{\cdot}H_2O + 3Ca(OH)_2 = 3CaO{\cdot}SiO_2{\cdot}3H_2O + H_2O \quad (3)$$

DN6 coagulates relatively fast (33.0 h), this is because part of the hemicellulose and a small amount of cellulose in the alkali-modified straw fibers undergo alkaline hydrolysis, and the anticoagulant components (extracts) in fibers produce water-soluble monosaccharide substances [40], which are removed during washing, thus shortening the coagulation time of the SFCC paste. DN3 cement paste also coagulates very quickly (36.0 h). This is because the straw fibers modified by a pure acrylic emulsion made it possible for the fiber surface to be coated with an acrylic acid film, which has excellent water resistance, alkali resistance, and durability. The film can hinder the release rate of the extracts in straw fibers, thus reducing the anticoagulant effect of extracts on the process of cement hydration. Of all the SFCC paste of several modified straw fibers, DN4 sets the slowest (76.5 h). This is because although a hydrophobic film formed by silicone emulsion on the surface of straw fibers prevents external water from permeating into the interior of particles and is able to reduce the release rate of extracts to a certain extent, composed mainly of alkyl alkoxy silane, the silicone emulsion will hinder the hydration reaction of cement to some extent. Alkyl alkoxy silanes hinder the hydration of cement due to the dehydration and condensation of ≡Si-OH formed by hydrolysis of silane functional groups with hydroxyl groups on the surface of cement particles. A hydrophobic adsorption layer is formed on the surface of cement particles and hydrates by chemical binding, which hinders the diffusion contact between mineral phase, water, and ions, thus delaying the hydration heat release process of cement [41].

The setting rate of DN5 of the modified-water straw fibers was also very slow (59.0 h). This is because although the water-modified straw fibers have dissolved some soluble organic monosaccharides in fibers and removed most extracts affecting cement hydration, they do not remove the extracts as thoroughly as the alkali-modified fibers. Parts of the extracts remaining in the fibers still affect the hydration process of the SFCC paste.

3.3. Effect of Modification Methods on Hydration Characteristics of SFCC. The hydration characteristics of SFCC refer to the process of temperature changing with time, which may be expressed with a time-temperature curve (see Figure 4) due to the exothermic hydration of cement when the mixture of straw fibers and cement-based material paste is stirred evenly. The evaluation of hydration characteristics of SFCC can reflect the evaluation of the compatibility between straw fibers and cement-based materials. The main evaluation indexes are as follows: the highest temperature of hydration heat T, the time reaching the highest temperature t, and the compatibility coefficient CA. CA is the ratio of hydration heat of the straw fiber cement paste to that of the pure cement paste within 24 hours, that is, the ratio of the area enclosed by the time-temperature curve and the time axis of the two. The higher the T, the shorter the t, the bigger the CA, and the better the compatibility between straw fibers and cement-based materials. The test results obtained from Figure 4 are shown in Figure 5. Under the conditions of this experiment, the compatibility between straw fibers and cement-based materials is mainly related to the magnitude of the fiber water absorption and the degree of release of the blocking components inside fibers. The mass water absorption of straw fibers within 24 h is shown in Table 5.

As shown in Figure 4, DR0 of the base paste without straw fibers reaches the highest hydration temperature peak after 13 hours, and the corresponding temperature of the temperature peak is 18.3%. The hydration exothermic rate of the SFCC paste with a fiber group tends to be gentle, and the exothermic peak decreases, but the peak time of the exothermic peak is 7 to 11.5 hours earlier than that of DR0. This is not inconsistent with the conclusion that the setting time of the paste mixed with straw fiber groups in Figure 3 is longer than that of the base group. The reason for this

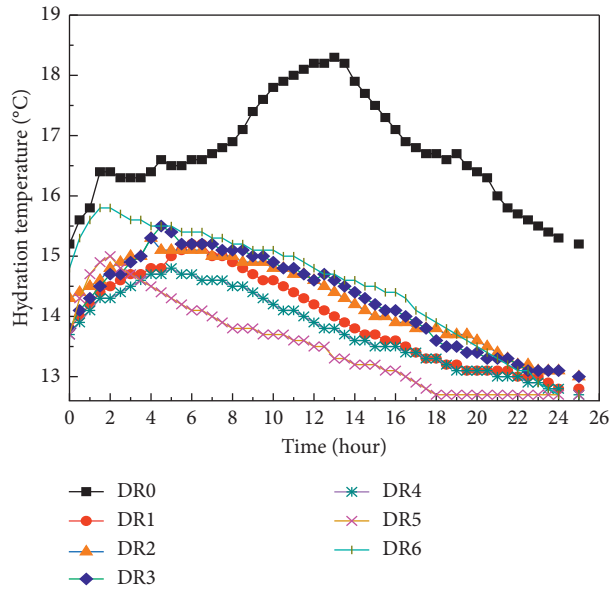

Figure 4: Test result of hydration temperature of the SFCC paste.

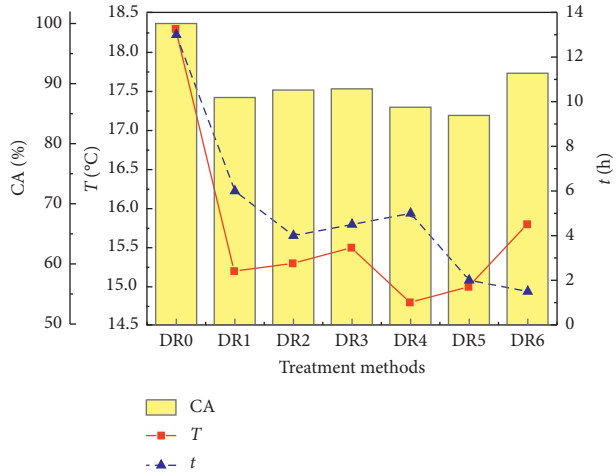

Figure 5: Test result of evaluation indexes of the compatibility between straw fibers and cement-based materials.

Table 5: Mass water absorption of the straw fiber within 24 h (%).

No.	0.5 h	1 h	2 h	3 h	5 h	6 h	12 h	24 h	Average
DS1	367.2	368.8	355.6	361.2	361.4	364.0	364.0	366.4	363.6
DS2	352.4	326.8	314.6	325.8	320.4	334.0	326.8	332.2	329.1
DS3	359.2	336.2	330.4	335.0	331.8	338.4	345.6	352.6	341.2
DS4	341.2	342.6	349.2	350.4	339.8	352.4	353.2	360.0	348.6
DS5	384.2	400.6	402.6	390.8	380.6	391.6	399.2	407.2	394.6
DS6	409.2	414.2	421.4	397.8	403.4	410.0	412.2	417.2	410.7

phenomenon is that, on the one hand, at the initial stage of cement hydration, with the total amount of water used basically unchanged, due to a high water absorption (see Table 5, the average water absorption of several straw fibers is 329.13%–410.68% within 24 hours), straw fibers absorb part of mixing water, causing the SFCC paste water-binder ratio to decrease, thus accelerating the setting and hardening of the cement [11, 42]. At the same time, the straw fibers saturated with absorbed water release a certain amount of extracts, which, having a good dispersing effect on cement particles, enlarge the water-cement effective contact area and accelerate the cement hydration reaction [9, 43]. Therefore, the hydration rate of the SFCC paste is faster than that of DR0, and the maximum hydration temperature peak time is ahead. On the other hand, the addition of straw fibers relatively reduces the amount of

cement in the mixture per unit volume, resulting in reduction of the cement hydration heat release. In addition, in the middle and later stages of hydration reaction, though modified, the straw fibers will unavoidably release some residual extracts in the alkaline environment of cement hydration, thus hindering, to a certain degree, the process of cement hydration and reducing the rate of hydration heat release. Therefore, the highest hydration temperature peak of several SFCC paste is still significantly lower than that of DR0.

In addition to the DR0 paste in Figure 5, of several SFCC pastes, the pastes with the highest hydration temperature peaks are DR6 (15.8°C), DR3 (15.5°C), and DR2 (15.3°C); the pastes that quickly attain the temperature peaks are DR6 (1.5 h), DR5 (2.0 h), and DR2 (4.5 h); the pastes with greater CA are DR6 (91.72%), DR3 (89.12%), and DR2 (88.93%). Comparing the test results of indexes T, CA, and t of the compatibility evaluation of SFCC paste hydration process, for the purpose of improving the compatibility between straw fibers and cement-based materials, the most recommended straw fiber modification methods are alkali modification (DR6), followed by acrylic emulsion modification (DR3) and $Na_2O{\cdot}nSiO_2$ modification (DR2).

3.4. Effect of Modification Methods on Chemical Structure of Straw Fibers. Fourier transform infrared spectroscopy (FTIR) can be used to detect the changes of functional groups of straw fibers before and after modification. The FTIR spectra of unmodified and modified straw fibers are shown in Figure 6 [44–48].

In Figure 6, the positions of main absorption peaks and corresponding functional groups of unmodified fibers DG1 are position 3427 cm^{-1} is the stretching vibration of intermolecular associative hydroxyl (-OH) of cellulose; 2918 cm^{-1} is the C-H stretching vibration of cellulose-saturated alkyl; 1636 cm^{-1} and 1516 cm^{-1} are the benzene ring skeleton C=C stretching vibration related to lignin; 1425 cm^{-1} is the wood-related methylene C-H antisymmetrical bending vibration peak; 1242 cm^{-1} lignin-related phenyl hydroxyl C-O stretching vibration; 1161 cm^{-1} asymmetrical out-of-plane stretching vibration of the C-O-C ether bond related to microcellulose and hemicellulose; 1057 cm^{-1} bending vibration related to polysaccharide cellulose and C-C-O stretching vibration; 897 cm^{-1} is lignin-related C-H bending vibration.

DG2–DG5 shows a decrease in the -OH stretching vibration peak at 3427 cm^{-1} corresponding to DG1, indicating a decrease in many associative hydroxyl groups; a slight decrease was observed in the peak values at 2918 cm^{-1} corresponding to DG1, indicating a slight decrease in the relative content of cellulose. The absorption peaks of DG2 disappeared at 1516 cm^{-1} and 897 cm^{-1} corresponding to DG1, indicating that the benzene ring structure of lignin decreased. The peak values of DG3, DG4, and DG5 at 1636 cm^{-1} to 1057 cm^{-1} corresponding to DG1 reduced to varying degrees. The changes of DG2, DG3, and DG4 patterns show that the film of $Na_2O{\cdot}nSiO_2$, pure acrylic acid polymer, and hydrophobic organosiloxane on the surface of straw fibers reduces the contact between cellulose and outside water. The film can plug the pores on the surface of straw fibers and increase the surface density of the fibers, which also means a relative reduction in the content of hemicellulose and lignin, a slight increase in the content of cellulose, an increase in the crystallinity of the fibers [49], and a reduction in the hydrophilicity of the fibers, thereby improving the compatibility between the fibers and cement-based materials. The changes of DG5 patterns show that, in the case of water-modified fibers, as viewed from the angle of the change in their chemical structure, part of hemicellulose and lignin decreased with the dissolution of some simple carbohydrates and the water absorption rate should also decrease. Form a physical point of view, in the water modification process, with the removal of water extracts, cellulose molecular chains are subjected to damage to a certain extent and more pores and defects are exposed on the surface of the fibers (see Figure 2), thus causing the water absorption of the fibers to increase to some extent, and the increase of water absorption caused by the physical damage to the fiber surface is often greater than that caused by the change of the chemical structure of fibers. The average water absorption (394.60%) of DS5 fibers within 24 h shown in Figure 3 also verified the correctness of the above analysis.

Compared with DG1, the peak height of DG6 increased at 3427 cm^{-1}, indicating an increase in hydrogen-bonded association -OH with cellulose, meaning an increase in the fiber water absorption. The main reasons for the increase of water absorption of the DG6 fiber are as follows: NaOH solution hydrolyzes the waxy layer on the surface of straw fibers into higher fatty acids and higher fatty alcohols and then destroys the waxy layer on the surface [50, 51]; when the metal hydrated ions in the NaOH solution enter the cellulose and interact with hydrogen bonds on the cellulose chain, it destroys some crystalline region of cellulose, decreasing the crystallinity of cellulose [52, 53]. On the other hand, the absorption peak of DG6 sees a significant increase at 2918 cm^{-1} corresponding to DG1, but disappears at 1516 cm^{-1} and 1242 cm^{-1} and diminishes at 1057 cm^{-1}, indicating that the content of cellulose increased, the content of lignin decreased, and the crystallinity of the fibers increased after modification with the NaOH solution. It also means it helps the water absorption of the fibers to reduce. Similar to the water modification, with the removal of alkali extracts in the process of alkali modification, the damage caused to cellulose and lignin molecular chains is greater than that of water-modified fibers, resulting in more exposed pores and defects on the fiber surface, thus greatly increasing the fiber water absorption. And this kind of water absorption increase caused by the physical damage is often dominant. The above analysis can be verified from the data in Table 5 where DS6 has higher water absorption than DS5.

3.5. Effect of Modification Methods on Mechanical Properties of SFCC. The test results of flexural and compressive strength of SFCC specimens mixed with unmodified and modified straw fibers at different ages are shown in Figure 7.

As shown in Figure 7, except for the 28 d strength of SFCC specimens DQ4 of the straw fibers modified with

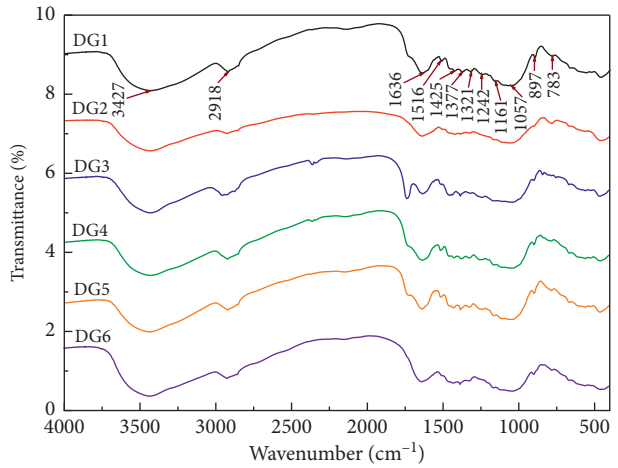

Figure 6: FTIR spectra of straw fibers modified with different methods.

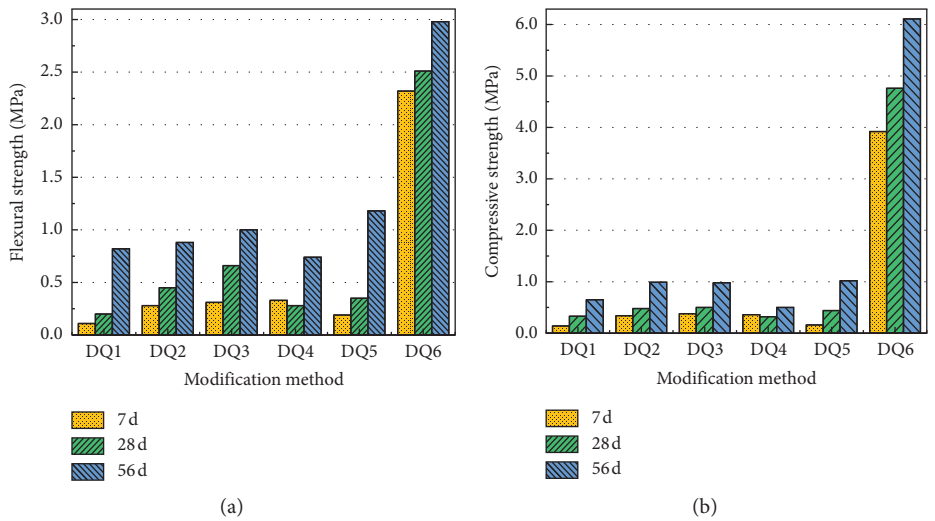

Figure 7: Strength of SFCC: (a) flexural strength; (b) compressive strength.

silicone waterproof emulsion, the strength of SFCC specimens of several modified straw fibers increased with the increase of age. In addition to DQ4, the flexural and compressive strength of the other four modified SFCC specimens were higher than that of the unmodified SFCC specimens. The flexural and compressive strength of the SFCC specimens DQ6 of alkali modified fibers were the highest at the early and middle-later stages, and the strength was significantly higher than that of the SFCC specimens of other modified fibers, of which 7 d flexural and compressive strength were 2.32 MPa and 3.92 MPa, 28 d 2.51 MPa and 4.76 MPa, and 56 d 2.98 MPa and 6.11 MPa, respectively. Except for DQ6, the higher 28 d strength was pure acrylic emulsion-modified fiber SFCC specimens DQ3 and again was $Na_2O{\cdot}nSiO_2$-modified fiber SFCC specimens DQ2. Besides DQ6, the better 56d strength was the water modified fiber SFCC test piece DQ5, again DQ3 and DQ2. The strength of DQ4 was not stable, 7 d strength was rather high, and 28 d strength decreased, and 56 d strength was even lower than that of DQ1. The strength of DQ5 was relatively low at the early stage, but its strength grew faster at the middle and later stages. The strength of 56 d was next only to that of DQ6.

The results in Figure 7 are also related to the fiber water absorption and the compatibility between straw fibers and cement-based materials. From the point of view of water absorption, the unmodified fiber DQ1 has high water absorption, the average water absorption of 24 h being 363.6% (see Table 5). When the mixture of SFCC reaches the same consistency, the water consumption increases. After the cement-based material hardens, it leaves large pores on the fiber surface where there is water, which reduces the mechanical properties of SFCC. In addition, there are problems of wet swelling and drying shrinkage for the straw fibers with high water absorption, which will lead to the change in volume of straw fibers, affecting the adhesion between fibers and cement-based materials, thereby the strength of DQ1 is not satisfactory.

However, the water absorption of modified straw fibers DQ2 and DQ3 is lower than that of DQ1. The average water

absorption of DQ2 and DQ3 was 34.5% and 22.4% lower than that of unmodified straw fibers, respectively (see Table 5). Therefore, with the mixing fluidity kept basically unchanged, the amount of water needed was less, and, when SFCC mixture hardened, the amount of evaporated water or bleeding quantity decreased, formation of capillary channels and pores decreased, and the effective cross section of the SFCC resisting load decreases less, which helps to improve the mechanical properties of SFCC and enhance the bond strength between straw fibers and cement-based materials.

From the point of view of the compatibility between fibers and cement-based materials, the strength of DQ1 is not high because extracts in straw fibers exert an anticoagulant effect on cement. However, DQ2 and DQ3 straw fibers, having a coated layer on their surfaces, which in turn can hinder the extracts release, will improve the compatibility between the fibers and cement-based materials. Similarly, DQ5 and DQ6 straw fibers also improve the compatibility between the fibers and cement-based materials due to removal of the extracts out of fibers. The strength of DQ5 is obviously lower than that of DQ6 because the removal of extracts from DQ5 straw fibers is not as complete as that of DQ6.

The strength of DQ4 is not stable, and it is even lower than that of DQ1 at the later stage, of which main reason is that the silane emulsion in the silicone waterproof emulsion retards the hydration of cement. In addition, the silane molecular hydrophobic film coated on the straw fiber surface, which though has the effect of decreasing the water absorption, the average mass water absorption within 24 hour is 15.0% which is lower than that of the unmodified fibers (see Table 5), will reduce the bonding properties of straw fibers with hardened cement-based materials, thereby the later strength of SFCC specimens declines to a certain extent.

To sum up, to improve the strength of SFCC, the most recommended modification methods of straw fibers are the alkali modification, followed by the pure acrylic emulsion and $Na_2O{\cdot}nSiO_2$ modification, and the water modification is also worth recommending.

3.6. Effect of Modification Methods on Hydrates of SFCC. The results of XRD analysis of SFCC 28 d-age hydrates are shown in Figure 8. As shown in Figure 8, several SFCC hydration products show crystalline diffraction peaks. The shape of the diffraction peaks and the location of the main peaks are generally similar, indicating that that the main phase types of several SFCC crystalline hydration products are basically the same, but the content of each phase and the type of individual phase are different. Several SFCC crystalline hydration products are mainly composed of clinker minerals that are not fully hydrated, such as tricalcium silicate [$Ca_3(SiO_4)O$], dicalcium silicate [$Ca_2(SiO_4)$], and hydrated crystalline minerals. The main phase hydrated calcium silicate gel (C-S-H) of hydration products of cement-based materials is not shown in the map due to its poor crystallinity.

In terms of phase types of crystalline hydration products, the hydration products of the unmodified straw fiber DX1

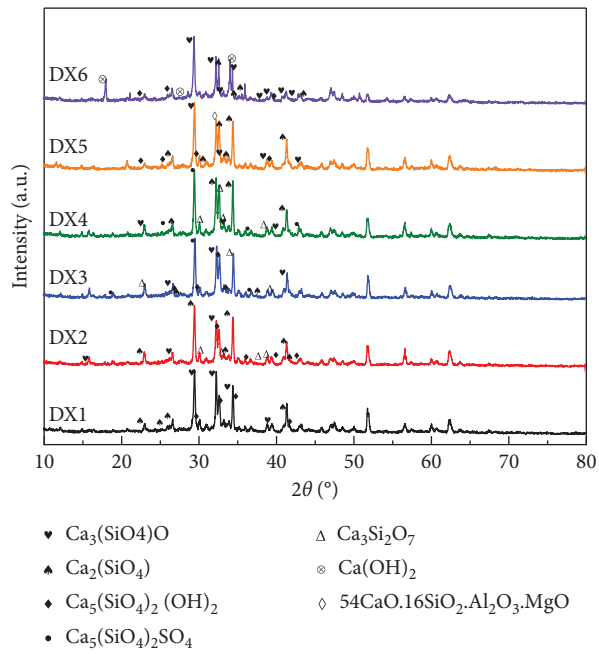

Figure 8: XRD spectra of hydrates of SFCC.

mainly include tricalcium silicate [Ca_3 (SiO_4) O], dicalcium silicate [Ca_2 (SiO_4)], calcium hydroxide [Ca_5 (SiO_4)$_2$ (OH)$_2$], and calcium silicate [$Ca_3Si_2O_7$]. The types of hydration products of SFCC blended with modified straw fibers are basically the same as DX1 or there are other minerals such as siderite [Ca_5 (SiO_4)$_2SO_4$], calcium magnesium aluminosilicate [54CaO. 16SiO_2 $Al_2O_3{\cdot}MgO$], and hydroxyapatite [Ca (OH)$_2$].

In terms of phase content of crystalline hydrates, according to the phase identification and analysis by Jade software and combined with the relevant literature [54–59], the diffraction peak area of each phase and the relative content of total amount of hydration products of SFCC are shown in Table 6. It can be seen from Table 6 that from the relative content of total hydration products, the relative content of total hydration products mixed with the unmodified fiber DX1 is the lowest and the relative content of total hydration products mixed with modified straw fiber DX2–DX6 is higher than that of DX1. The largest relative content of the total hydration products is DX2, which is 120.03%, and the least relative content of the total hydration products is DX4, which is 108.76%.

The above analysis shows that because the thin layer on the fiber modifier surfaces hinders the release of extracts and a small amount of modifier components may be involved in the cement hydration reaction (for spray modification), or a certain amount of extracts are removed out of fibers (for dip modification), the modified straw fibers are able to decrease the inhibitory effect of anticoagulant components in fibers on SFCC hydration process, for types and relative contents of crystalline phases in the hydration products of SFCC mixed with modified straw fibers were significantly higher than that of SFCC mixed with unmodified straw fibers, thus revealing the intrinsic reason why the coagulation and hardening rate of SFCC mixed

Table 6: The diffraction peak area of each phase and the relative content of total hydration products of SFCC.

No.	$Ca_3(SiO_4)O$	$Ca_2(SiO_4)$	$Ca_5(SiO_4)_2(OH)_2$	$Ca_3Si_2O_7$	$Ca_5(SiO_4)_2SO_4$	$54CaO{\cdot}16SiO_2{\cdot}Al_2O_3{\cdot}MgO$	$Ca(OH)_2$	Total area	Relative content (%)
DX1	251.01	168.39	153.80	80.15	—	—	—	499.55	100.00
DX2	136.84	291.63	122.32	48.82	—	—	—	599.61	120.03
DX3	172.07	33.96	109.50	98.24	131.55	—	—	545.32	109.16
DX4	46.10	239.78	—	118.84	138.62	—	—	543.33	108.76
DX5	146.45	285.77	41.98	—	—	99.47	—	573.66	114.84
DX6	294.99	82.76	58.97	—	—	—	106.85	543.57	108.81

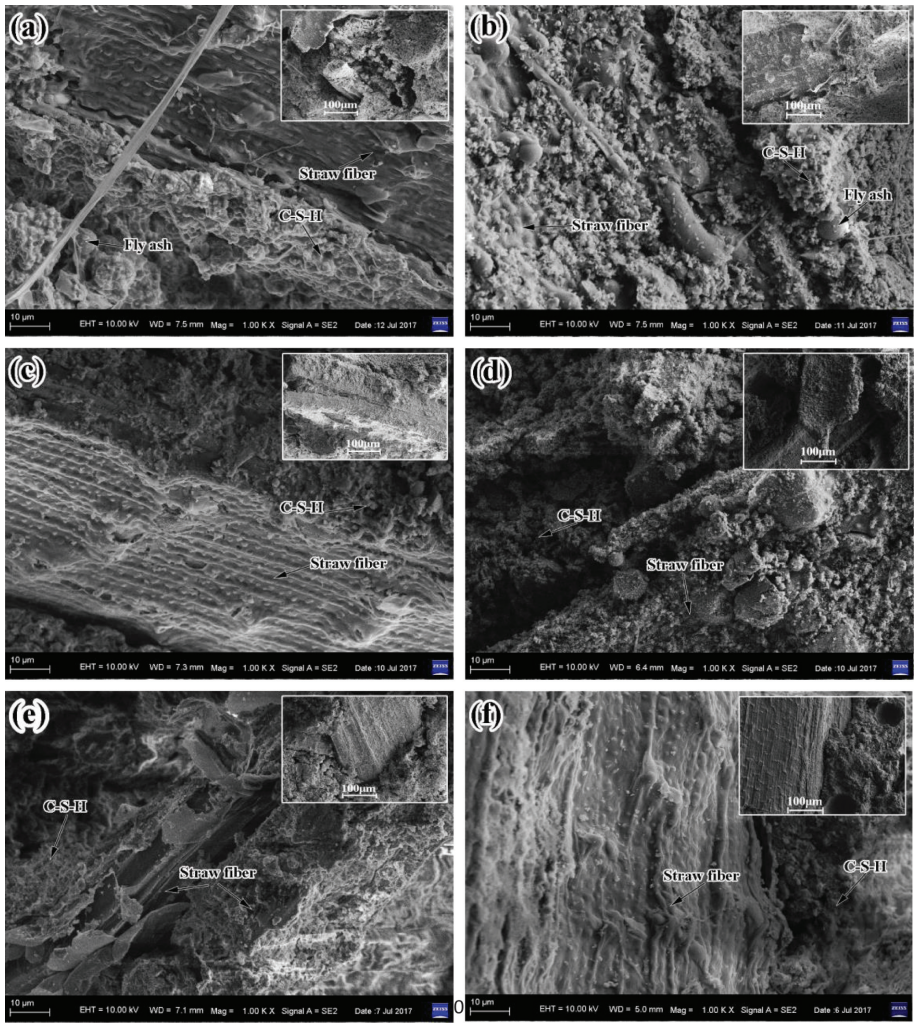

Figure 9: SEM images of SFCC (1000 times).

with modified straw fibers in Figure 3 were faster than that of SFCC mixed with unmodified straw fibers.

3.7. Effect of Modification Methods on the Microstructure of SFCC. In order to observe the microstructure of hydrates of SFCC of 28 d age, i.e., to see both the overall distribution of hydrates and the bonding states of straw fibers and hydrates (especially C-S-H gel), SEM diagrams of 1000 times and 6000 times were used for analysis, respectively, as shown in Figures 9 and 10.

As shown in Figures 9 and 10, the hydrates of SFCC appear in flocculent, short rod, granular, and fibrous forms and shapes, of which main components are C-S-H, crystalline hydrates, unhydrated minerals, and unhydrated particles (fly ash, fibrous scraps, etc.) These hydrates wrap around the straw fibers and form accumulation bodies in the outer layer of the fibers. It can be seen from Figures 9(a) and 10(a) that the hydrates of SFCC blended with unmodified straw fibers take on massive accumulations and between the hydrates there are fly ash particles which are not involved in cement hydration and the internal structure of the hydrates

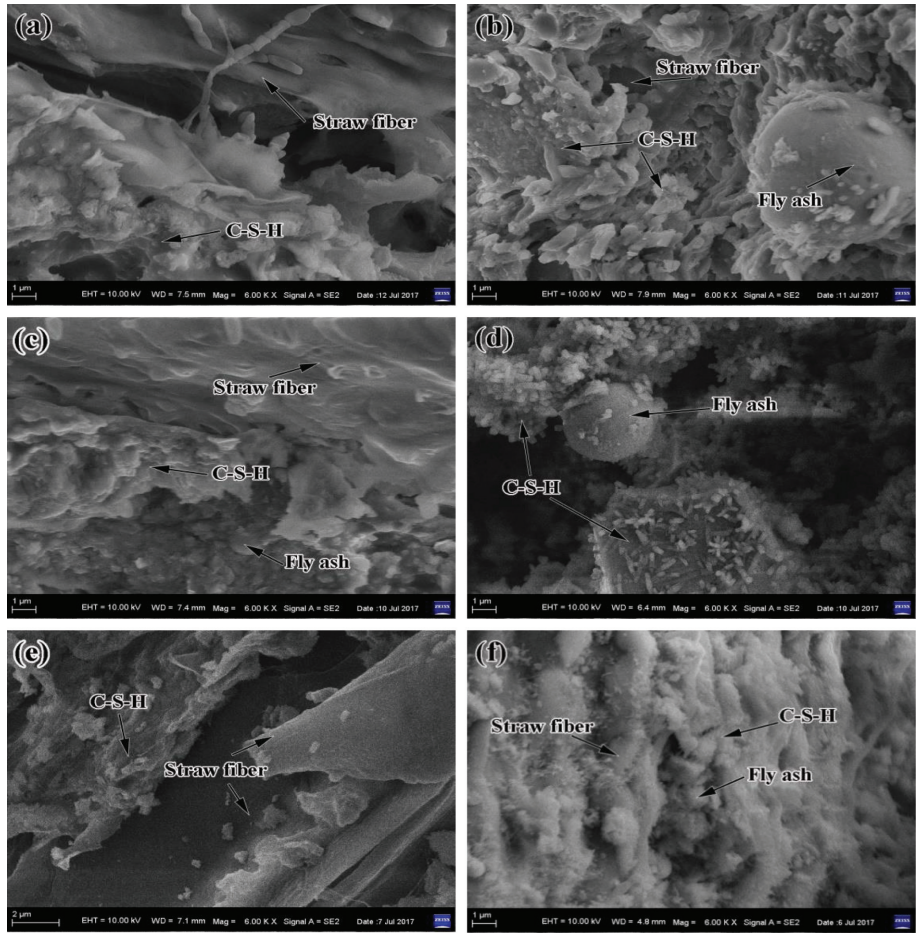

Figure 10: SEM images of SFCC (6000 times).

is loose and the porosity is large. The bonding between fibers and cement-based materials is relatively loose, and there is a significant number of voids (see the illustration). As shown in Figures 9(b), 10(b), 9(c), and 10(c), the amount of hydrates of the SFCC mixed with $Na_2O{\cdot}nSiO_2$-modified fibers and the SFCC mixed with pure acrylic emulsion-modified fibers is significantly higher than that of Figures 9(a) and 10(a), with improved the interfacial structure between fibers and cement-based materials and a tight bond between the two phases. From Figures 9(d) and 10(d), it is shown that there is a loose connection between hydrate bulks of SFCC mixed with silicone waterproof emulsion-modified fibers, with poor integrity of hydrates, large porosity, and inadequate bond between fibers and cement-based materials. The results of Figures 9(e) and 10(e) show that the hydrates of SFCC blended with water-modified fibers have a compact structure, but there are some cracks and voids in it, the fiber surface is partially damaged with scraps, and there is an inadequate bond between the fibers and cement-based materials. From the results of Figures 9(f) and 10(f), it can be seen that there are gels with rather small particles and fly ash with deep hydration between the SFCC hydrates blocks mixed with alkali-modified fibers, with a very close overall structure, and a satisfactory bond between the fibers and the cement-based material.

From the above analysis of Figures 9 and 10, it can be seen that the final hydrates of SFCC in (e), (c), and (b) have a compact structure and a close bond between straw fibers and cement-based materials, of which corresponding fiber modification methods are alkali, pure acrylic emulsion, and $Na_2O{\cdot}nSiO_2$ modifications. The analysis also reveals that the three kinds of modified fiber SFCC paste have a fast setting and hardening rate, high hydration temperature, satisfactory compatibility between fibers and cement-based materials, and more types or quantities of hydrates, and high mechanical properties after hardening. Therefore, the results of Figures 9 and 10 validate the analysis of the fiber modification effect, and the difference of micromorphology of several SFCC hydrates is precisely the ultimate embodiment of difference in compatibility between modified straw fibers and cement-based materials.

4. Conclusion

Through analysis of the chemical structure and microstructure of straw fibers before and after modification, the setting time and hydration characteristics of the SFCC paste, the mechanical properties of SFCC specimens, and the hydrates and micromorphology of SFCC specimens, this paper has illuminated the effect of modified straw fibers on

the compatibility between fibers and cement-based materials and has reached the following conclusions:

(1) The compatibility between straw fibers and cement-based materials could be effectively improved by modifying straw fibers. The setting time of the modified straw fiber SFCC paste was shorter than that of the unmodified straw fiber SFCC paste. The best fiber modification method to improve the setting time of SFCC paste was $Na_2O{\cdot}nSiO_2$ modification.

(2) The modified method of straw fiber to improve the strength of SFCC was alkali modification, followed by pure acrylic emulsion and $Na_2O{\cdot}nSiO_2$ modification, and water modification method was also recommended.

(3) Based on the test results of the three compatibility evaluation indexes T, CA, and t of SFCC paste hydration process, the alkali modification was the most recommended one to improve the compatibility between straw fibers and cement-based materials, followed by the pure acrylic acid emulsion and $Na_2O{\cdot}nSiO_2$ modifications.

(4) Several methods of modifying straw fiber were mainly employed to reduce the fiber water absorption by decreasing -OH associated with the cellulose hydrogen bond or increasing the crystallinity of fibers to improve the compatibility between fibers and cement-based materials.

Data Availability

The datasets generated and analyzed during the currentstudy are available from the corresponding author on reasonable request.

Conflicts of Interest

The authors declare no conflicts of interest.

Acknowledgments

The authors gratefully acknowledged financial supports from the Beijing Natural Science Foundation of China (project no. 2172021), National Natural Science Foundation of China (project no. 41772335), 13th Five-Year National Key R&D Program "Research on Facilities Hazard Monitoring and Landslide Early Warning Standards" (project no. 2018YFF0213304), National Key R&D Program (project no. 2016YFC0701810), and Innovative Engineering-Integration and Demonstration: Key Technology R&D Projects for Improving the Resilience Capability of Urban Rail Transit Infrastructure Disasters (project no. 2018-1).

References

[1] L. Lavagna, S. Musso, G. Ferro, and M. Pavese, "Cement-based composites containing functionalized carbon fibers," *Cement and Concrete Composites*, vol. 88, pp. 165–171, 2018.

[2] L. Sun, Q. Hao, J. Zhao, D. Wu, and F. Yang, "Stress strain behavior of hybrid steel-PVA fiber reinforced cementitious composites under uniaxial compression," *Construction and Building Materials*, vol. 188, pp. 349–360, 2018.

[3] A. Abrishambaf, M. Pimentel, and S. Nunes, "Influence of fibre orientation on the tensile behaviour of ultra-high performance fibre reinforced cementitious composites," *Cement and Concrete Research*, vol. 97, pp. 28–40, 2017.

[4] M. Cao, Y. Mao, M. Khan, W. Si, and S. Shen, "Different testing methods for assessing the synthetic fiber distribution in cement-based composites," *Construction and Building Materials*, vol. 184, pp. 128–142, 2018.

[5] H. Li, R. Mu, L. Qing, H. Chen, and Y. Ma, "The influence of fiber orientation on bleeding of steel fiber reinforced cementitious composites," *Cement and Concrete Composites*, vol. 92, pp. 125–134, 2018.

[6] Q.-B. Wang, Q.-K. Zhu, T.-S. Shao et al., "The rheological test and application research of glass fiber cement slurry based on plugging mechanism of dynamic water grouting," *Construction and Building Materials*, vol. 189, pp. 119–130, 2018.

[7] M. Cao and L. Li, "New models for predicting workability and toughness of hybrid fiber reinforced cement-based composites," *Construction and Building Materials*, vol. 176, pp. 618–628, 2018.

[8] K. Tang, "Stray current induced corrosion of steel fibre reinforced concrete," *Cement and Concrete Research*, vol. 100, pp. 445–456, 2017.

[9] O. Onuaguluchi and N. Banthia, "Plant-based natural fibre reinforced cement composites: a review," *Cement and Concrete Composites*, vol. 68, pp. 96–108, 2016.

[10] M. Ardanuy, J. Claramunt, and R. D. Toledo Filho, "Cellulosic fiber reinforced cement-based composites: a review of recent research," *Construction and Building Materials*, vol. 79, pp. 115–128, 2015.

[11] X. Xie, Z. Zhou, M. Jiang, X. Xu, Z. Wang, and D. Hui, "Cellulosic fibers from rice straw and bamboo used as reinforcement of cement-based composites for remarkably improving mechanical properties," *Composites Part B: Engineering*, vol. 78, pp. 153–161, 2015.

[12] S. L. M. R. Filho, P. R. Oliveira, L. M. G. Vieira, T. H. Panzera, R. T. S. Freire, and F. Scarpa, "Hybrid bio-composites reinforced with sisal-glass fibres and Portland cement particles: a statistical approach," *Composites Part B*, vol. 149, pp. 58–65, 2018.

[13] H. Ahmad and M. Fan, "Interfacial properties and structural performance of resin-coated natural fibre rebars within cementitious matrices," *Cement and Concrete Composites*, vol. 87, pp. 44–52, 2018.

[14] M. U. Farooqi and M. Ali, "Contribution of plant fibers in improving the behavior and capacity of reinforced concrete for structural applications," *Construction and Building Materials*, vol. 182, pp. 94–107, 2018.

[15] B. Çomak, A. Bideci, and Ö Salli Bideci, "Effects of hemp fibers on characteristics of cement based mortar," *Construction and Building Materials*, vol. 169, pp. 794–799, 2018.

[16] M. R. Ahmad, B. Chen, S. Y. Oderji, and M. Mohsan, "Development of a new bio-composite for building insulation and structural purpose using corn stalk and magnesium phosphate cement," *Energy and Buildings*, vol. 173, pp. 719–733, 2018.

[17] H. Li, M. Dai, S. Dai, and X. Dong, "Current status and environment impact of direct straw return in China's cropland—a review," *Ecotoxicology and Environmental Safety*, vol. 159, no. 15, pp. 293–300, 2018.

[18] H. Liu, X. Ou, J. Yuan, and X. Yan, "Experience of producing natural gas from corn straw in China," *Resources, Conservation and Recycling*, vol. 135, pp. 216–224, 2018.

[19] X. Wang, L. Yang, Y. Steinberger, Z. Liu, S. Liao, and G. Xie, "Field crop residue estimate and availability for biofuel production in China," *Renewable and Sustainable Energy Reviews*, vol. 27, no. 11, pp. 864–875, 2013.

[20] X. Zeng, Y. Ma, and L. Ma, "Utilization of straw in biomass energy in China," *Renewable and Sustainable Energy Reviews*, vol. 11, no. 5, pp. 976–987, 2007.

[21] M. Ramesh, K. Palanikumar, and K. H. Reddy, "Plant fibre based bio-composites: sustainable and renewable green materials," *Renewable and Sustainable Energy Reviews*, vol. 79, no. 11, pp. 558–584, 2017.

[22] D. Jiang, S. Cui, F. Xu, and T. Tuo, "Impact of leaf fibre modification methods on compatibility between leaf fibres and cement-based materials," *Construction and Building Materials*, vol. 94, no. 30, pp. 502–512, 2015.

[23] G. Li, Y. Yu, J. Li, C. Li, and Y. Wang, "Research on adaptability between crop-stalk fibers and cement," *Cement and Concrete Research*, vol. 34, no. 7, pp. 1081–1085, 2004.

[24] R. Narendar and K. Priya Dasan, "Chemical treatments of coir pith: morphology, chemical composition, thermal and water retention behavior," *Composites Part B: Engineering*, vol. 56, pp. 770–779, 2014.

[25] S. Chakraborty, S. P. Kundu, A. Roy, B. Adhikari, and S. B. Majumder, "Polymer modified jute fibre as reinforcing agent controlling the physical and mechanical characteristics of cement mortar," *Construction and Building Materials*, vol. 49, pp. 214–222, 2013.

[26] J. Wei and C. Meyer, "Improving degradation resistance of sisal fiber in concrete through fiber surface treatment," *Applied Surface Science*, vol. 289, no. 1, pp. 511–523, 2014.

[27] J. Claramunt, M. Ardanuy, J. A. García-Hortal, and R. D. T. Filho, "The hornification of vegetable fibers to improve the durability of cement mortar composites," *Cement and Concrete Composites*, vol. 33, no. 5, pp. 586–595, 2011.

[28] D. M. Jiang and S. P. Cui, "Processing method of leaves used in thermal insulation building materials," *Advanced Materials Research*, vol. 538–541, pp. 1286–1289, 2012.

[29] D. Jiang and S. Cui, "Experimental study of design of mix proportion of leaf concrete," *Applied Mechanics and Materials*, vol. 174–177, pp. 1177–1183, 2012.

[30] M. Fan, M. K. Ndikontar, X. Zhou, and J. N. Ngamveng, "Cement-bonded composites made from tropical woods: compatibility of wood and cement," *Construction and Building Materials*, vol. 36, pp. 135–140, 2012.

[31] J. L. Pehanich, P. R. Blankenhorn, and M. R. Silsbee, "Wood fiber surface treatment level effects on selected mechanical properties of wood fiber-cement composites," *Cement and Concrete Research*, vol. 34, no. 1, pp. 59–65, 2004.

[32] Y. Diquélou, E. Gourlay, L. Arnaud, and B. Kurek, "Impact of hemp shiv on cement setting and hardening: influence of the extracted components from the aggregates and study of the interfaces with the inorganic matrix," *Cement and Concrete Composites*, vol. 55, pp. 112–121, 2015.

[33] M. Sood and G. Dwivedi, "Effect of fiber treatment on flexural properties of natural fiber reinforced composites: a review," *Egyptian Journal of Petroleum*, vol. 27, no. 4, pp. 775–783, 2018.

[34] Y. Zuo, J. Xiao, J. Wang, W. Liu, X. Li, and Y. Wu, "Preparation and characterization of fire retardant straw/magnesium cement composites with an organic-inorganic network structure," *Construction and Building Materials*, vol. 171, pp. 404–413, 2018.

[35] J. Gu and Y.-L. Hsieh, "Alkaline cellulose nanofibrils from streamlined alkali treated rice straw," *ACS Sustainable Chemistry & Engineering*, vol. 5, no. 2, pp. 1730–1737, 2017.

[36] F. Wang, S. Zhou, L. Li, and X. Zhang, "Changes in the morphological-mechanical properties and thermal stability of bamboo fibers during the processing of alkaline treatment," *Polymer Composites*, vol. 39, no. 3, pp. 1421–1428, 2018.

[37] Y. Zhou, M. Fan, and L. Chen, "Interface and bonding mechanisms of plant fibre composites: an overview," *Composites Part B: Engineering*, vol. 101, pp. 31–45, 2016.

[38] A. Sellami, M. Merzoud, and S. Amziane, "Improvement of mechanical properties of green concrete by treatment of the vegetals fibers," *Construction and Building Materials*, vol. 47, pp. 1117–1124, 2013.

[39] S. A. Bernal, J. L. Provis, V. Rose, and R. Mejía de Gutierrez, "Evolution of binder structure in sodium silicate-activated slag-metakaolin blends," *Cement and Concrete Composites*, vol. 33, no. 1, pp. 46–54, 2011.

[40] A. Oushabi, S. Sair, F. Oudrhiri Hassani, Y. Abboud, O. Tanane, and A. El Bouari, "The effect of alkali treatment on mechanical, morphological and thermal properties of date palm fibers (DPFs): study of the interface of DPF-polyurethane composite," *South African Journal of Chemical Engineering*, vol. 23, pp. 116–123, 2017.

[41] W. Fan, F. Stoffelbach, J. Rieger et al., "A new class of organosilane-modified polycarboxylate superplasticizers with low sulfate sensitivity," *Cement and Concrete Research*, vol. 42, no. 1, pp. 166–172, 2012.

[42] M.-A. Berthet, N. Gontard, and H. Angellier-Coussy, "Impact of fibre moisture content on the structure/mechanical properties relationships of PHBV/wheat straw fibres biocomposites," *Composites Science and Technology*, vol. 117, pp. 386–391, 2015.

[43] G. A. M. Brasileiro, J. A. R. Vieira, and L. S. Barreto, "Use of coir pith particles in composites with Portland cement," *Journal of Environmental Management*, vol. 131, pp. 228–238, 2013.

[44] T. Lu, S. Liu, M. Jiang et al., "Effects of modifications of bamboo cellulose fibers on the improved mechanical properties of cellulose reinforced poly(lactic acid) composites," *Composites Part B: Engineering*, vol. 62, pp. 191–197, 2014.

[45] F. Z. Arrakhiz, M. Elachaby, R. Bouhfid, S. Vaudreuil, M. Essassi, and A. Qaiss, "Mechanical and thermal properties of polypropylene reinforced with Alfa fiber under different chemical treatment," *Materials & Design*, vol. 35, pp. 318–322, 2012.

[46] S. P. Kundu, S. Chakraborty, A. Roy, B. Adhikari, and S. B. Majumder, "Chemically modified jute fibre reinforced non-pressure (NP) concrete pipes with improved mechanical properties," *Construction and Building Materials*, vol. 37, pp. 841–850, 2012.

[47] M. M. Kabir, H. Wang, K. T. Lau, F. Cardona, and T. Aravinthan, "Mechanical properties of chemically-treated hemp fibre reinforced sandwich composites," *Composites Part B: Engineering*, vol. 43, no. 2, pp. 159–169, 2012.

[48] Y. Seki, M. Sarikanat, K. Sever, and C. Durmuşkahya, "Extraction and properties of *Ferula communis* (chakshir) fibers as novel reinforcement for composites materials," *Composites Part B: Engineering*, vol. 44, no. 1, pp. 517–523, 2013.

[49] I. N. Grubeša, B. Marković, A. Gojević, and J. Brdarić, "Effect of hemp fibers on fire resistance of concrete," *Construction and Building Materials*, vol. 184, pp. 473–484, 2018.

[50] X. Xia, W. Liu, L. Zhou, Z. Hua, H. Liu, and S. He, "Modification of flax fiber surface and its compatibilization in polylactic acid/flax composites," *Iranian Polymer Journal*, vol. 25, no. 1, pp. 25–35, 2016.

[51] L. Y. Xiang, S. H. Hanipah, M. A. P. Mohammed, A. S. Baharuddin, and A. M. Lazim, "Microstructural, mechanical, and physicochemical behaviours of alkali pretreated oil palm stalk fibres," *Bioresources*, vol. 10, no. 2, pp. 2783–2796, 2015.

[52] Y. Luo, X. Pan, Y. Ling, X. Wang, and R. Sun, "Facile fabrication of chitosan active film with xylan via direct immersion," *Cellulose*, vol. 21, no. 3, pp. 1873–1883, 2014.

[53] M. D. Teli and J. M. Terega, "Effects of alkalization on the properties of Ensete ventricosum plant fibre," *The Journal of the Textile Institute*, vol. 110, no. 4, pp. 496–507, 2019.

[54] D. Jiang, S. Cui, X. Song, and J. Zhang, "Analysis of micromorphology and heat-insulating property of leaf concrete," *Construction and Building Materials*, vol. 49, pp. 663–671, 2013.

[55] E. Qoku, T. A. Bier, and T. Westphal, "Phase assemblage in ettringite-forming cement pastes: a X-ray diffraction and thermal analysis characterization," *Journal of Building Engineering*, vol. 12, pp. 37–50, 2017.

[56] L. H. J. Martin, F. Winnefeld, E. Tschopp, C. J. Müller, and B. Lothenbach, "Influence of fly ash on the hydration of calcium sulfoaluminate cement," *Cement and Concrete Research*, vol. 95, pp. 152–163, 2017.

[57] G. V. P. Bhagath Singh and K. V. L. Subramaniam, "Quantitative XRD study of amorphous phase in alkali activated low calcium siliceous fly ash," *Construction and Building Materials*, vol. 124, pp. 139–147, 2016.

[58] P. Ghoddousi and L. Adelzade Saadabadi, "Study on hydration products by electrical resistivity for self-compacting concrete with silica fume and metakaolin," *Construction and Building Materials*, vol. 154, pp. 219–228, 2017.

[59] L. Wang, Y. Dong, S. H. Zhou, E. Chen, and S. W. Tang, "Energy saving benefit, mechanical performance, volume stabilities, hydration properties and products of low heat cement-based materials," *Energy and Buildings*, vol. 170, pp. 157–169, 2018.